

Title	Zero Forcing and Decision Feedback Detectors in MIMO Communication Channels and Their Applications to Frequency-Overlapped Multi-Carrier Signaling
Author(s)	MATSUMOTO, Tadashi
Citation	IEICE Transactions on Communications, E83-B(10): 2386-2393
Issue Date	2000-10-20
Type	Journal Article
Text version	publisher
URL	http://hdl.handle.net/10119/4683
Rights	Copyright (C)2000 IEICE. Tadashi Matsumoto, IEICE Transactions on Communications, E83-B(10), 2000, 2386-2393. http://www.ieice.org/jpn/trans_online/
Description	

PAPER

Zero Forcing and Decision Feedback Detectors in MIMO Communication Channels and Their Applications to Frequency-Overlapped Multi-Carrier Signaling

Tadashi MATSUMOTO[†], *Regular Member*

SUMMARY This paper investigates noise enhancement factors of a zero-forcing detector and a decision feedback detector for synchronous Multiple Input Multiple Output (MIMO) channels. It is first shown that the zero-forcing and decision feedback detectors can be implemented in a vector digital filter form, and the noise enhancement factors with the detectors can easily be calculated by using the vector digital filter form. This paper then applies the zero-forcing and decision feedback detectors to the signal detection of a frequency-overlapped multicarrier signaling (FOMS) system. The normalized noise enhancement factor, which is given as a product of the noise enhancement and bandwidth reduction factors, is shown to be smaller with the decision feedback detector than the zero-forcing detector. Results of computer simulations conducted to evaluate bit error rate (BER) performances with the two detectors are also shown together with the BER performance with a conventional channel-by-channel detector.

key words: MIMO channel, multichannel signal detection, interference cancellation, zero forcing detector, decision feedback detector

1. Introduction

Communication systems have long been based on the Single-Input Single-Output (SISO) concept which is how multiple users' signals accommodated in a system should be made, at high level, independent of each other. In frequency- or time-division multiple access schemes, entire portion of frequency or time, respectively, are divided into slots, and the slots are assigned to multiple users to maintain the signal orthogonality among the users. Even in code division multiple access (CDMA) systems, where the same frequency band is shared by multiple users, the despreading process at receiver suppresses other simultaneous users' signals, thereby each user's signal can be detected independently of other users.

Recently, the Multi-Input Multi-Output (MIMO) communication concept has been recognized as potential principle that can significantly enhance spectrum efficiency of communication systems over the SISO systems. In communications over MIMO channel, not only can it be a severe problem that inter-symbol interference (ISI) causes distortion on the symbol of interest,

but also inter-channel interference (ICI) distorts the symbol. Therefore, elimination of the ISI and ICI components from the symbol of interest is a key to achieving significant spectrum efficiency enhancement over SISO systems while keeping communication quality reasonable.

Several ISI and ICI cancellation techniques have been presented in a couple of literatures. Reference [1] derives an optimal detector based on the minimum mean square error (MMSE) criterion, and Ref. [2] a zero-forcing detector for MIMO channels. Reference [3] showed that a decision feedback detector can be derived from the spectral factorization of the MIMO channel's matrix transfer function. However, issues related to the spectrum efficiencies of systems based on the MIMO communication concept have not yet been discussed.

The signal processing for the zero-forcing detector is equivalent to the inverse processing of the matrix transfer function. Similarly to zero-forcing ISI equalizers, it suffers from severe noise enhancement [4]. The decision feedback detector also suffers from the noise enhancement. A goal of the first half of this paper is to analyze the noise enhancement factors of the zero-forcing and decision feedback MIMO channel detectors. Vector digital filter forms of the zero-forcing and decision feedback detectors are derived. It is then shown that the noise enhancement factors can easily be calculated by using the vector digital filter form of the detectors.

The latter half of this paper applies the zero-forcing and the decision feedback detectors to the signal detection of a frequency-overlapped multicarrier system (FOMS) [5], which is a frequency division multiplexing technique, but spectra of the multiple subcarrier signals are intentionally overlapped with each other. The purpose of the overlapping is to reduce the entire bandwidth, while keeping the total information bit rate transmitted kept constant. This should lead to a spectrum efficiency enhancement over without overlapping*.

The logical input-output relationship of the frequency-overlapped multicarrier system can be viewed as that of the MIMO system. Hence, elimination of ISI and ICI is a key to achieving the purpose. In fact, the zero-forcing and decision feedback detectors

Manuscript received January 5, 2000.

Manuscript revised March 29, 2000.

[†]The author is with NTT Mobile Communications Network Inc., Yokosuka-shi, 239-8536 Japan.

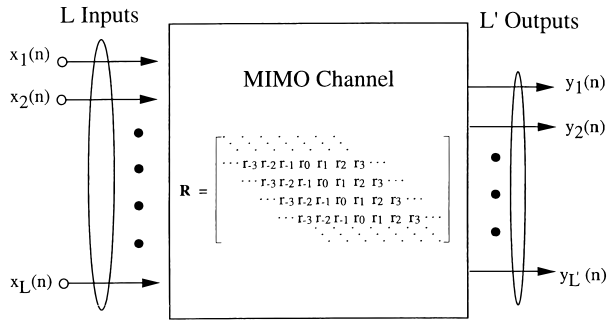


Fig. 1 MIMO communication system model.

incur noise enhancement, and hence how much portion of spectra should be overlapped depends on the tradeoff between the bandwidth reduction and noise enhancement factors.

This paper is organized as follows. Section 2 shows the MIMO channel model used in this paper, and describes mathematical expressions for each component of the model. Section 3 derives a vector digital filter form of the zero-forcing and decision feedback detectors. It is then shown that the noise enhancement factor with the zero-forcing detector can easily be calculated by using the vector digital filter form. Section 4 applies the zero-forcing and the decision feedback detectors to the signal detection of frequency-overlapped multicarrier signaling. Spectrum efficiency of the system normalized by the bandwidth reduction and noise enhancement factors are then properly defined. Section 5 presents results of numerical calculations for the noise enhancement factors and the normalized spectrum efficiencies with the detectors.

2. System Model

As shown in Fig. 1, MIMO communication systems have multiple inputs and outputs. Let the input vector be denoted, in time domain, by

$$\mathbf{x}(n) = [x_1(n)x_2(n)\cdots x_L(n)]^t \quad (1)$$

with L being the number of the inputs. Let the output vector be denoted by

$$\mathbf{y}(n) = [y_1(n)y_2(n)\cdots y_{L'}(n)]^t \quad (2)$$

with L' being the number of the outputs. In this paper $L = L'$ is assumed. In MIMO systems, $\mathbf{y}(n)$ is affected by $\mathbf{x}(n)$ input to the transmitter at past, present, and future symbol timings.

Symbol timing synchronism among signals on the L channels is assumed. Therefore, the input-output relationship can, in time domain, be expressed as

$$\mathbf{Y} = \mathbf{R}\mathbf{X} + \mathbf{N}, \quad (3)$$

where \mathbf{Y} and \mathbf{X} are vectors with infinite dimension, given by $\mathbf{Y} = [\bullet\bullet\bullet, \mathbf{y}(n-1)^t, \mathbf{y}(n)^t, \mathbf{y}(n+1)^t, \bullet\bullet\bullet]^t$ and

$\mathbf{X} = [\bullet\bullet\bullet, \mathbf{x}(n-1)^t, \mathbf{x}(n)^t, \mathbf{x}(n+1)^t, \bullet\bullet\bullet]^t$, respectively, and $\mathbf{N} = [\bullet\bullet\bullet, \mathbf{n}(n-1)^t, \mathbf{n}(n)^t, \mathbf{n}(n+1)^t, \bullet\bullet\bullet]^t$ is a sequence of the noise vector $\mathbf{n}(n) = [n_1(n), n_2(n), \bullet\bullet\bullet, n_L(n)]^t$. The matrix \mathbf{R} also has infinite dimension, and is given by

$$\mathbf{R} = \begin{bmatrix} \ddots & \ddots \\ \cdots & r_{-3} & r_{-2} & r_{-1} & r_0 & r_1 & r_2 & r_3 & \cdots & \\ & \cdots & r_{-3} & r_{-2} & r_{-1} & r_0 & r_1 & r_2 & r_3 & \cdots \\ & & \cdots & r_{-3} & r_{-2} & r_{-1} & r_0 & r_1 & r_2 & r_3 & \cdots \\ & & & \cdots & r_{-3} & r_{-2} & r_{-1} & r_0 & r_1 & r_2 & r_3 & \cdots \\ & & & & \ddots \end{bmatrix} \quad (4)$$

where $r_n = \{h_{kl}(n)\}$, $n \in (-\infty, +\infty)$, is an $L \times L$ submatrix whose kl -element $h_{kl}(n)$ represents the k -th channel's overall response to the impulse input to the l -th channel at the symbol timing $t = nT$. The terms $h_{kl}(n)$ with $n < 0$, $n = 0$, and $n > 0$ correspond to the l -to- k response to the input at past, present, and future symbol timings, respectively.

Taking the z -transform of Eq. (4), we have the z -domain representation of the input/output relationship as

$$\mathbf{Y}(z) = \mathbf{F}(z)\mathbf{X}(z) + \mathbf{N}(z), \quad (5)$$

where $\mathbf{F}(z)$ is the matrix transfer function given by

$$\mathbf{F}(z) = r_0 + \sum_{n=1}^{\infty} [r_{-n}z^{-n} + r_nz^n], \quad (6)$$

and $\mathbf{Y}(z)$, $\mathbf{X}(z)$, and $\mathbf{N}(z)$ are, respectively, the z -transforms of $\mathbf{y}(n)$, $\mathbf{x}(n)$ and $\mathbf{n}(n)$. Since the overall transfer function of the Nyquist roll-off filter is shared equally by transmitter and receiver, the z -transform of the covariance matrix $\langle \mathbf{n}(\bullet)\mathbf{n}^H(\bullet+m) \rangle$ is equal to $\sigma^2 \mathbf{F}(z)$ with $\langle |n_k(n)|^2 \rangle = \sigma^2$ for $1 \leq k \leq L$.

3. Detectors

3.1 Zero-Forcing Detector

Zero-forcing detector for the MIMO channel performs upon the received vector sequence $\mathbf{y}(n)$ the signal processing corresponding to the inverse filter $G(z) = \mathbf{F}^{-1}(z)$ of the matrix transfer function. Assuming the nonsingularity[†] of the submatrix r_0 , $\mathbf{F}^{-1}(z)$ can be expanded into an infinite series as

[†]Careful design of signal waveform should make it hold that even though some portion of signal spectra overlap with each other, but orthogonality holds among the signals at every symbol timing. This is the case of orthogonal-frequency division multiplexing (OFDM) [6]. However, a correlation property among the signals, which may be suitable for MIMO channel detectors, may be brought about also by a careful waveform design. Design of signal waveform is out of the scope of this paper.

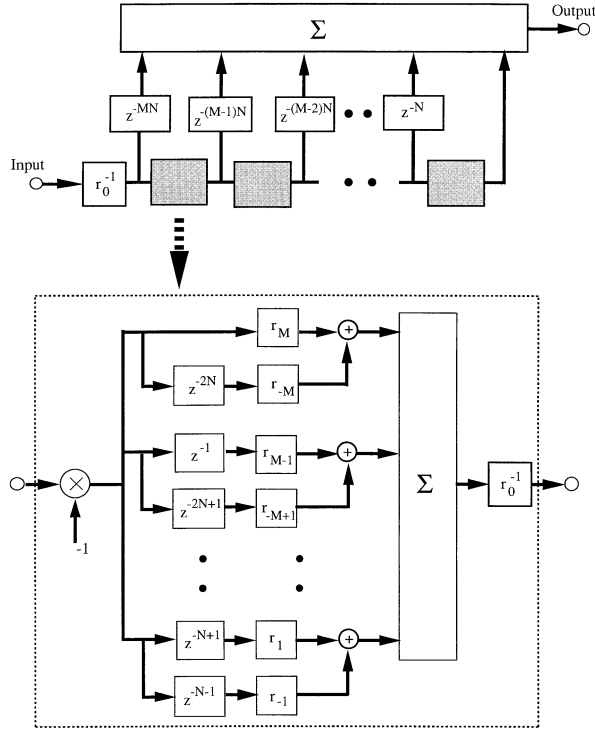


Fig. 2 Causal approximation of zero-forcing detector.

$$G(z) = F(z)^{-1} = \sum_{m=0}^{\infty} (-1)^m \left\{ r_0^{-1} \sum_{n=1}^{\infty} (r_{-n} z^{-n} + r_n z^n) \right\}^m r_0^{-1}. \quad (7)$$

Equation (7) has terms of z^n with $n > 0$ which correspond to noncausal components in the inverse filter's impulse response. In practice, at the cost of appreciable performance degradation, these noncausal components can be truncated after an appropriate delay. In fact, Eq. (7) can be approximated by a causal filter

$$z^{-MN} G(z) \cong \sum_{m=0}^M (-1)^m z^{-(M-m)N} \cdot \left\{ r_0^{-1} \sum_{n=1}^N (r_{-n} z^{-(N+n)} + r_n z^{-(N-n)}) \right\}^m r_0^{-1} \quad (8)$$

with MN denoting the delay for the truncation, which indicates that the impulse response of the approximated inverse filter has length of $2MN + 1$.

A block diagram of the signal processing required to implement the approximated zero-forcing detector given by Eq. (8) is shown in Fig. 2. Obviously, it can be implemented in the form of a vector digital filter whose implementation does not require the inverse of the matrix rational transfer function: it only requires the inverse of r_0 .

As in zero-forcing equalizers [4] for ISI cancella-

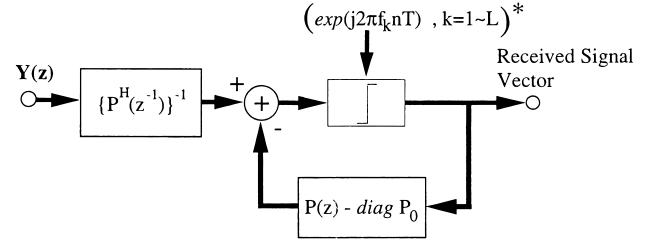


Fig. 3 Block diagram of decision feedback detector.

* This portion is effective only when the detector is applied to FOMS.

tion, the noise vector $\mathbf{n}_Z(n) = [n_{Z1}(n), n_{Z2}(n), \dots, n_{ZL}(n)]^t$ at the inverse filter output is somewhat enhanced as a result of inverse filtering. The z -transform of the covariance matrix $\langle \mathbf{n}_Z(\bullet) \mathbf{n}_Z^H(\bullet + m) \rangle$ is equal to $\sigma^2 F^{-1}(z)$ since, with the z -transform of $\langle \mathbf{n}(\bullet) \mathbf{n}^H(\bullet + m) \rangle$ being $F(z)$, $G(z) = F^{-1}(z)$ [8]. Therefore, $n_{Zk}(n)$ is a zero-mean Gaussian random variable with variance $\sigma^2 [G_0]_{kk}$ with

$$G(z) = F^{-1}(z) = G_0 + \sum_{n=1}^{\infty} [G_{-n} z^{-n} + G_n z^n]. \quad (9)$$

Hence, the noise enhancement factor ν_k with the k -th channel is given by $\nu_k = [G_0]_{kk}$. ν_k can be calculated numerically as the response at timing $n = MN$ of the approximated inverse filter to the input vector $\mathbf{x}(0) = [x_1(0), x_2(0), \dots, x_L(0)]^t$ with $x_k(0) = 1$ and the rest of the elements being 0 [9].

3.2 Decision Feedback Detector

Decision feedback detector counts on the fact that for each channel both the transmitter and receiver use root Nyquist roll-off filters having the same transfer function. Therefore, the overall matrix transfer function $F(z)$ is a spectrum matrix that can be factored as [7]

$$F(z) = P^H(z^{-1})P(z) \quad (10)$$

with

$$P(z) = \sum_{i=0}^{\infty} P_{-i} z^{-i}, \quad (11)$$

where, with P_0 being lower triangular, $P(z)$ and $P^{-1}(z)$ are both causal and stable matrix filters.

A block diagram of the decision feedback detector is shown in Fig. 3. With this configuration, the feedforward filter is $\{P^H(z^{-1})\}^{-1}$ which whitens the noise components $\mathbf{n}(n)$. The feedback filter

$$B(z) = P(z) - \text{diag}\{P_0\} \quad (12)$$

is strictly causal and eliminates ICI components due

[†]In synchronous systems, r_0 becomes singular if the waveforms on some of the L channels are not linearly independent. Otherwise, r_0 is likely to be nonsingular.

to past symbols [8]. Again, the feedforward filter $\{P^H(z^{-1})\}^{-1}$ is highly noncausal, for which its implementation requires approximation.

As in the zero-forcing detector, the decision feedback detector suffers from noise enhancement. The noise enhancement factor for the k -th channel with the MIMO decision feedback detector can be derived in the same way as the factor for CDMA decision feedback multiuser detector is derived [3]. It is given by $\nu_k = 1/[P_0]_{kk}^2$, derivation of which is straightforward. A vector digital filter approximation of $\{P^H(z^{-1})\}^{-1}$ can easily be derived. Using the vector digital filter approximation, $[P_0]_{kk}$ can be calculated in the same way as $[G_0]_{kk}$, was derived for the zero-Forcing detector. Error propagation is another error cause that should be taken into account when evaluating its real performance. However, it is difficult to theoretically analyze the effect of error propagation on overall performance, and the theoretical derivation of the bit error rate (BER) with the decision feedback detector exceeds the scope of this paper.

4. Application to Frequency-Overlapped Multicarrier Signaling

In this section, the MIMO concept is applied to frequency-overlapped multicarrier signaling, which is a frequency division multiplexing technique, but spectra of the multiple subcarrier signals are intentionally overlapped with each other. The purpose of the overlapping is to reduce the entire bandwidth, while keeping the total information bit rate transmitted kept constant. This should lead to a spectrum efficiency enhancement over without overlapping.

4.1 Transmitter

Figure 4 shows a block diagram of the transmitter and receiver in the equivalent complex baseband domain. There are L subcarriers in this system. It is assumed that the L subcarriers' symbol timings are synchronized to each other. The k -th subcarrier is modulated by the symbol sequence $s_k(n)$ to be transmitted where $n \in (-\infty, +\infty)$ is the symbol timing index. $s_k(n) (= I_k + jQ_k)$, where I_k and Q_k are the in-phase and quadrature components, respectively, takes one of the signal points defined as a modulation alphabet.

The symbol sequence $s_k(n)$ is multiplied by a complex carrier $\exp\{j\omega_k t\}$ where $\omega_k = 2\pi f_k$, and bandpass-filtered for spectrum shaping. The center frequency of the k -th subcarrier's bandpass filter is f_k . It is assumed that the overall transfer function of the Nyquist roll-off filter is shared equally by transmitter and receiver, and hence the equivalent lowpass version of the bandpass filter is the root Nyquist roll-off filter. The composite signal $Z_t(t)$ comprised of the L filtered modulated subcarriers can then be expressed as

$$Z_t(t) = \sum_{k=1}^L Z_{mk}(t), \tag{13}$$

where $Z_{mk}(t)$ is the bandpass filter's response waveform to the modulated subcarrier $Z_{tk}(t) = s_k(n) \bullet \exp\{j\omega_k t\}$. This complex composite signal is up-converted and transmitted.

4.2 Receiver

The output $Z_{rk}(t)$ of the k -th subcarrier's bandpass filter, which is equivalent to the root Nyquist roll-off receiver filter, is sampled at each symbol timing nT . If noise is absent, the sampled bandpass filter output $y_k(n) = Z_{rk}(nT)$ is equal to the k -th bandpass filter output sample in response to the sequence $\mathbf{x}(n)$, $n \in (-\infty, +\infty)$, of the input vector $\mathbf{x}(n) = [x_1(n), x_2(n), \dots, x_L(n)]$ with $x_k(n) = s_k(n) \bullet \exp\{j\omega_k nT\}$. Hence, the input-output relationship of this system is given by Eqs. (1)–(4) derived for MIMO channels.

Note that the kl -element $h_{kl}(n)$ of $L \times L$ submatrix $r_n = \{h_{kl}(n)\}$ represents the k -th subcarrier's overall response to the impulse input to the l -th subcarrier at the symbol timing $t = nT$. The terms $h_{kl}(n)$ with $n < 0$, $n = 0$, and $n > 0$ correspond to the l -to- k response to the input at past, present, and future symbol timings, respectively. For $n < 0$, $h_{kl}(n) \neq 0$ since the Nyquist roll-off filter is not causal. Note further that with $k = l$, the overall response $h_{kk}(n)$ of the bandpass filter is

$$h_{kk}(n) = \begin{cases} \exp\{j\omega_k nT\}, & n = 0, \\ 0, & n \neq 0. \end{cases} \tag{14}$$

The zero-forcing detector for the FOMS system can be derived in a straightforward manner from the one for the MIMO channel. The inverse filter output samples are multiplied by the conjugated complex subcarriers $\exp\{-j\omega_k nT\}$ to obtain M received baseband signals $r_k(n)$. Decisions are then made on $r_k(n)$ based upon the modulation format used. Alternatively, for each subcarrier the decision region itself may be rotated which corresponds to multiplying the complex subcarrier $\exp\{j\omega_k nT\}$ at the transmitter and the decisions are made directly on the inverse filter output samples. These two methods are equivalent in the zero-forcing detector, however, as shown in Fig. 3, the latter form of making decision process is effectively used in the decision feedback detector: the signal points in the modulation format multiplied by the complex subcarriers $\exp\{j\omega_k nT\}$ are the inputs to the feedback filter.

As described in Sect. 3.1, the zero-forcing and decision feedback detectors suffer from noise enhancement. However, the overlapping reduces the entire system bandwidth. Hence, a reasonable measure of the overall spectrum efficiency for the k -th subcarrier is the product $\nu_k \eta$ of the noise enhancement factor ν_k and the bandwidth reduction factor η given by

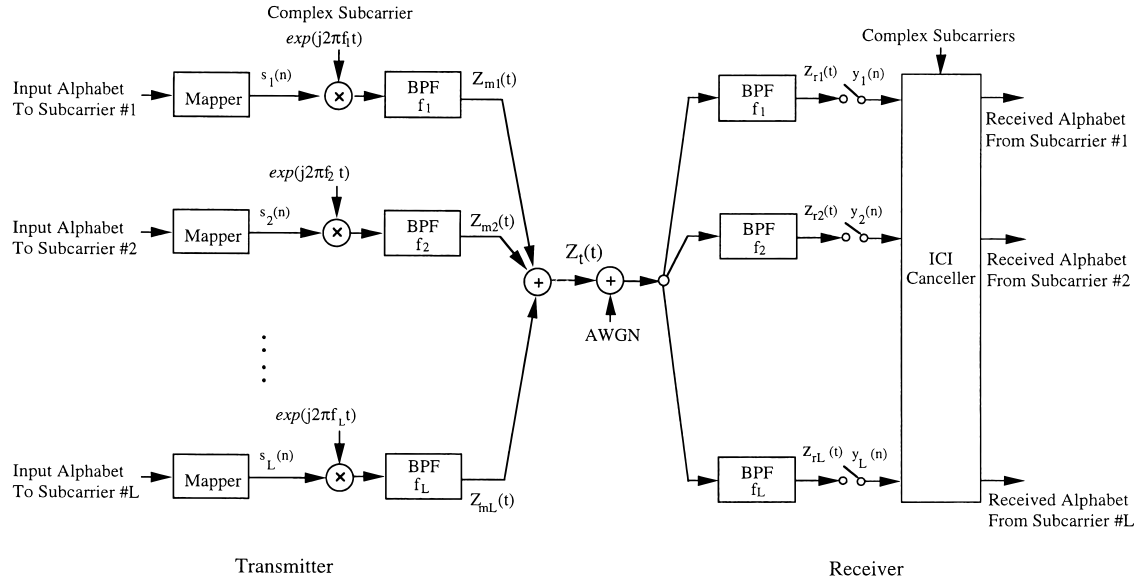


Fig. 4 Block diagram of FOMS system.

$$\eta = \frac{1 + \alpha}{1 + \alpha_0} \cdot \frac{L(1 - f_{ov}) + f_{ov}}{L}, \quad (15)$$

where $f_{ov} = 1 - \Delta f T / (1 + \alpha)$ is the overlapping ratio with α being the rolloff factor. α_0 is the rolloff factor used in a reference multicarrier signaling system without overlapping. A positive gain in overall spectrum efficiency is achieved over the reference system with $\nu_k \eta < 1$. Section 4 shows the results of numerical calculations for $\nu_k \eta$.

5. Numerical Calculations

This section shows results of numerical calculations for the zero-forcing and decision feedback FOMS detectors' performances. The noise enhancement factors with the zero-forcing and decision feedback detectors, and their normalized version, normalized by the bandwidth reduction factor, are used as a performance measures. Bit error rate (BER) performances with the detectors as well as a conventional detector which makes decisions on received signal samples subcarrier-by-subcarrier are also presented.

5.1 Asymptotic Performance

Figure 5 shows, for the number of subcarriers $L = 3$ and the rolloff factor $\alpha = 0.5$, the noise enhancement factor ν_k , $k = 1-3$, versus the overlapping ratio f_{ov} . A general observation of these curves is that noise enhancement increases with f_{ov} . This is reasonable because when f_{ov} increases, more ICI components from symbols farther in time and frequency appear on the symbol of interest. It is found that for the decision feedback detector, increasing subcarrier index k decreases the noise enhancement factor. This is not the case for the zero-forcing detector where the noise enhancement with the

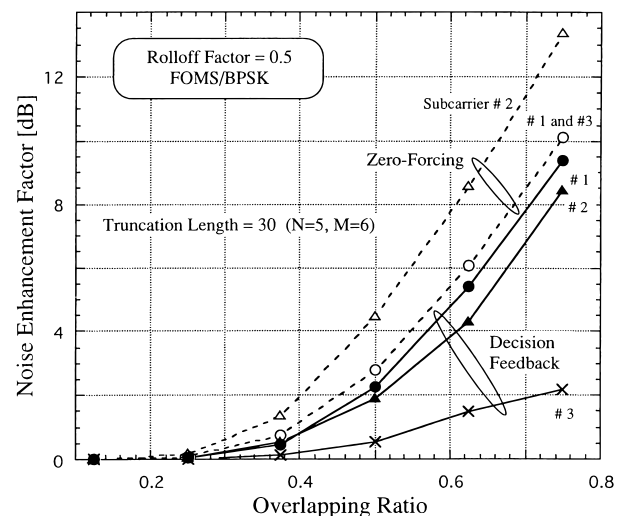


Fig. 5 Noise enhancement factor.

subcarrier on the center frequency band is larger than those with the subcarriers on both sides.

The cyclic use of all subcarriers should achieve average performances supported by the averaged noise enhancement factor. Figure 6 shows for $\alpha = 0.5$ and $L = 3$ the averaged noise enhancement factor ν versus the overlapping ratio f_{ov} . The bandwidth reduction factor is also plotted. It is found that for the decision feedback detector, the averaged noise enhancement is balanced by the bandwidth reduction when the overlapping ratio f_{ov} is about 0.5. For the zero-forcing detector, the balance point is $f_{ov} = 0.4$.

Figures 7(a) and (b) show for the zero-forcing and decision detectors, respectively, the averaged normalized noise enhancement factor $\eta \nu$, averaged over the subcarriers, versus the overlapping ratio f_{ov} with α

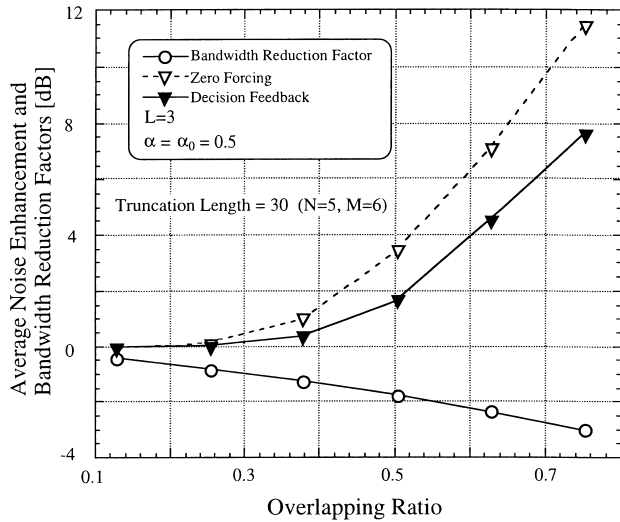


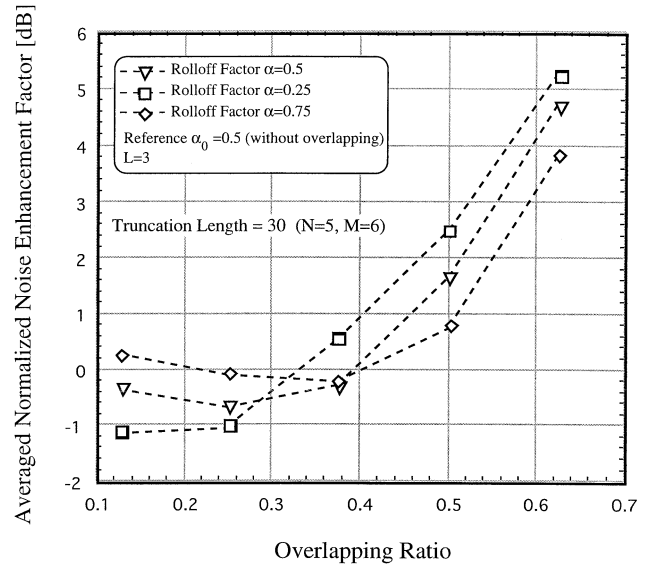
Fig. 6 Bandwidth reduction and averaged noise enhancement factors.

as a parameter ($\alpha_0 = 0.5$ and $L = 3$). It is found that for the decision feedback detector, positive gains in overall spectrum efficiency over the $\alpha_0 = 0.5$ reference system without overlapping can be achieved with the overlapping ratio being roughly $f_{ov} \leq 0.45$, $f_{ov} \leq 0.5$ and $0.2 \leq f_{ov} \leq 0.54$, respectively, for $\alpha = 0.25$, 0.5 and 0.75 . For the zero-forcing detector, the ranges for positive gain are roughly $f_{ov} \leq 0.34$, $f_{ov} \leq 0.4$ and $0.2 \leq f_{ov} \leq 0.4$, respectively, for $\alpha = 0.25$, 0.5 and 0.75 , which are relatively small compared with those for the decision feedback detector.

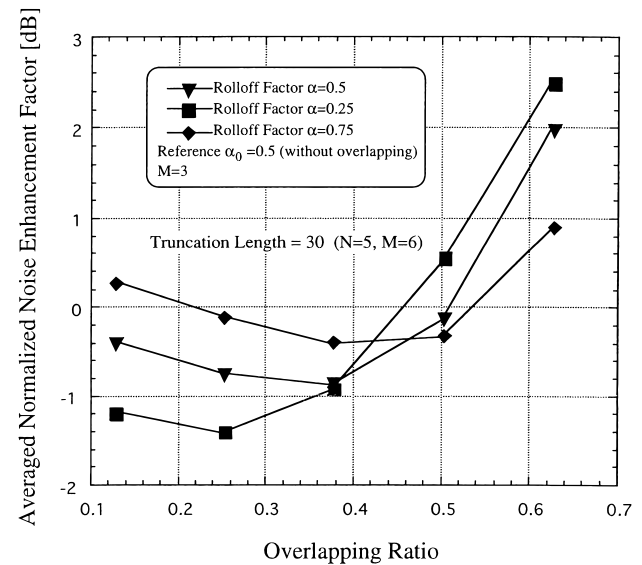
5.2 BER Performance

The BER performances with the zero-forcing and decision feedback detectors were evaluated through computer simulations in the additive white Gaussian noise (AWGN) channel. Binary phase shift keying (BPSK) was assumed as the modulation scheme. The values of the overlapping parameters are $L = 3$, $f_{ov} = 0.375$ and $\alpha = 0.5$. The BER performance with a conventional detector was also evaluated where each subcarrier makes its own signal detection independently of other subcarriers. The results are shown in Figs. 8(a) and (b): Fig. 8(a) is for the 1st and the 3rd subcarriers, and Fig. 8(b) for the 2nd subcarrier. The theoretical BPSK coherent detector's BER curve is also plotted for comparison. It is found that the BER's with the zero-forcing and decision feedback detectors are much better than that with the conventional detector, even though they suffer from noise enhancement.

The noise enhancement factor values for the zero-forcing detector are 0.88 dB for the 1st and the 3rd subcarriers, and 1.62 dB for the 2nd subcarrier. For the decision feedback detector the values are 0.54 dB, 0.44 dB and 0.14 dB for the 1st, 2nd and 3rd subcarriers, respectively. The curves in Figs. 8(a) and (b) slightly differ



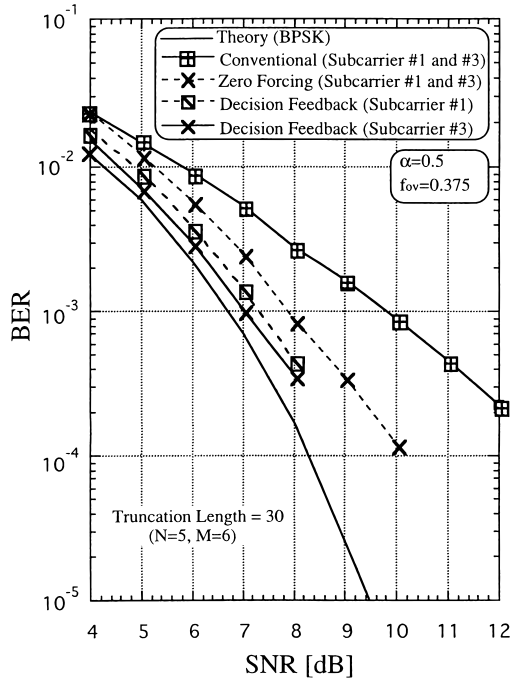
(a)



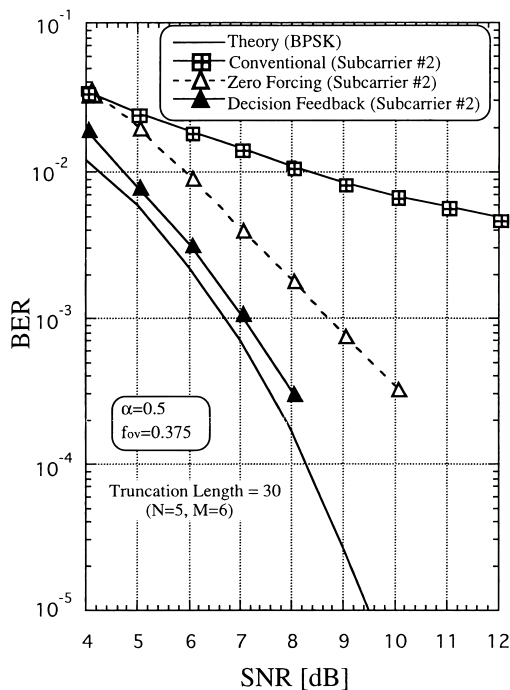
(b)

Fig. 7 (a) Averaged normalized noise enhancement factor with zero-forcing detector. (b) Averaged normalized noise enhancement factor with decision feedback detector.

from the asymptotic performance curves generated by shifting the theoretical BPSK BER curve by their corresponding noise enhancement factors. This may be due to the approximations made in the implementations of the detector algorithms such as the causal approximation of the inverse matrix transfer function of the zero forcing detector as well as the truncation of z 's terms of Eq. (8) in the derivation of the spectral factorization for the decision feedback detector. Effects of truncation are investigated in Ref. [9]. Another reason for this discrepancy, which is more essential than the computational truncation, is the fact that the noise enhancement factor is an asymptotic performance figure which



(a)



(b)

Fig. 8 (A) BER of subcarriers #1 and #3. (B) BER of subcarrier #2.

is approached by the BER curves when received SNR becomes large. The error propagation inherent within the decision feedback detector is another error cause that has not been taken into account in the asymptotic performance analysis. However, even in the presence of error propagation, the overall BER performance with

the decision feedback detector is much better than with the zero-forcing detector.

6. Conclusions

We have investigated the noise enhancement factors of the zero-forcing and decision feedback MIMO channel detectors in this paper. It has been shown that the zero-forcing and decision feedback detectors can be implemented in a vector digital filter form, and that the noise enhancement factors with the detectors can easily be calculated by using the vector digital filter. This paper then applied the zero-forcing and the decision feedback detectors to the signal detection of a frequency-overlapped multicarrier system. It has been shown that since the logical input-output relationship of the frequency-overlapped multicarrier system can be viewed as a MIMO system, detectors derived for MIMO channels can effectively eliminate ISI and ICI distortions on the subcarriers.

The zero-forcing and decision feedback detectors for the frequency-overlapped multicarrier system were then derived. Both the zero-forcing and the decision feedback detectors suffer from noise enhancement. It has been shown that for the decision feedback detector the normalized noise enhancement factor decreases as the subcarrier index increases. On the other hand, for the zero-forcing detector the noise enhancement of subcarriers on both sides of the frequency band is smallest.

The average normalized noise enhancement factor, averaged over all the subcarriers, is, in general, smaller with the decision feedback detector than with the zero-forcing detector if they have the same overlapping parameter values. Positive spectrum efficiency gains over a reference system without overlapping can be achieved in a wider range of the overlapping ratio with the decision feedback detector than with the zero-forcing detector.

The bit error rate performance with the detectors as well as the conventional subcarrier-by-subcarrier detector were also presented as an overall performance measure. It has been shown that the zero-forcing and decision feedback detectors achieve much better performances than the conventional detector under spectrum overlapping. The BER curves with the detectors were found to approach their corresponding asymptotic curves which were determined from the noise enhancement factors. This is because mainly of the approximations made when implementing the detector algorithms. The error propagation is another error cause for the decision feedback detector which, however, was not taken into account in the asymptotic performance analysis. It has been shown that even with the error propagation, the overall BER performance with the decision feedback detector is much better than with the zero-forcing detector.

For analysis simplicity, the nonfading additive

white Gaussian noise channel was assumed throughout this paper. However, it should be emphasized that the major results of this paper can easily be extended to fading channels by the proper use of channel estimation algorithms. Such investigations are left as future study.

References

- [1] A.R. Kaye and D.A. George, "Transmission of multiple PAM signals over multiple channel and diversity systems," *IEEE Trans. Commun.*, vol.COM-18, pp.520–526, Oct. 1970.
- [2] W. Van Etten, "An optimum linear receiver for multiple channel digital transmission systems," *IEEE Trans. Commun.*, vol.COM-23, pp.828–834, Aug. 1975.
- [3] A. Duel-Hallen, "A family of multiuser decision-feedback detectors for asynchronous code-division multiple-access channels," *IEEE Trans. Commun.*, vol.43, pp.421–434, April 1995.
- [4] J.G. Proakis, *Digital Communications*, McGraw-Hill, 1983.
- [5] T. Matsumoto and T. Asai, "Frequency-overlapped multi-carrier signaling with inter-carrier interference cancellation (FOLMSIC)," *IEICE Technical Report*, DSP97-135, Jan. 1998.
- [6] S.B. Weinstein and P.M. Ebert, "Data transmission by frequency division multiplexing using the discrete Fourier transform," *IEEE Trans. Commun.*, vol.COM-19, pp.628–634, Oct. 1971.
- [7] M.C. Davis, "Factoring the spectral matrix," *IEEE Trans. AC.*, pp.296–305, Oct. 1963.
- [8] R. Lupas and S. Verdú, "Near-far resistance of multiuser detectors in asynchronous channels," *IEEE Trans. Commun.*, vol.38, pp.496–508, April 1990.
- [9] T. Kawahara and T. Matsumoto, "Joint decorrelating multiuser detection and channel estimation in asynchronous CDMA mobile communications channels," *IEEE Trans. Veh. Technol.*, vol.44, pp.506–515, Aug. 1995.



Tadashi Matsumoto received his B.S., M.S., and Doctorate degrees in electrical engineering from Keio University, Yokohama-shi, Japan in 1978, 1980 and 1991, respectively. He joined Nippon Telegraph and telephone Corporation (NTT) in April 1980. From April 1980 to May 1987, he researched signal transmission technologies, such as modulation/demodulation schemes, as well as radio link design for mobile communications systems.

He participated in the R&D project of NTT's high-capacity mobile communications system, where he was responsible for the development of the base station transmitter/receiver equipment for the system. From May 1987 to February 1991, he researched error control strategies, such as Forward Error Correction (FEC), Trellis Coded Modulation (TCM), and Automatic Repeat Request (ARQ) in digital mobile radio channels. He developed an efficient new ARQ scheme suitable to the error occurrence in TDMA mobile signal transmission environments. He was involved in the development of a Japanese TDMA Digital Cellular Mobile Communications System. He took the leadership for the development of the facsimile and data communications service units for the system. In July 1992, he transferred to NTT Mobile Communications Network Inc. (NTT DoCoMo). From February 1991 to April 1994, he was responsible for research on Code Division Multiple Access (CDMA) mobile communications systems. He intensively researched multiuser detection schemes for multipath mobile communications environments. He was also responsible for research on error control schemes for CDMA Mobile communications systems. He concentrated on research of Maximum *A posteriori* probability (MAP) algorithm and its reduced complexity version for decoding of concatenated codes. From 1992 to 1994, he served as a part-time lecturer at Keio University. In April 1994, he moved to NTT America where he served as a senior technical advisor of the joint project with NTT and NEXTEL Communications. In March 1996, he returned to NTT DoCoMo, and since then he has been researching time-space signal processing for very high speed mobile signal transmission. Presently, he is an Executive Research Engineer at NTT DoCoMo. Since January of 1998, he has been serving as a secretary of IEEE Vehicular Technology Society Tokyo Chapter. He is a senior member of IEEE.